One-dimensional photonic crystal optical limiter

Boon Yi Soon and Joseph W. Haus

Electro-Optics Program, University of Dayton, Dayton, OH 45419-0245
boonyi@yahoo.com, jwhaus@udayton.edu

Michael Scalora

Weapons Science Directorate, AMSMI-RD-WS-ST, RD & EC, U.S. Army Missile Command, Building 7804, Redstone Arsenal, Alabama 35898-5000

Concita Sibilia

INFM at Dipartimento di Energetica, Università diRoma "La Sapienza", Via A. Scarpa, 16 I-00161 Rome, Italy

Abstract: We explore a new passive optical limiter design using transverse modulation instability in the one-dimensional photonic crystal (PC) using $\chi^{(3)}$ materials. The performance of PC optical limiters strongly depends on the choice of the materials and the geometry and it improves as the duration of the incident pulse is extended. PC optical limiter performance is compared with that of a device made from homogeneous material. We identify three criteria for benchmarking the PC optical limiter. We also include a discussion of the advantages and disadvantages of PC optical limiters for real world applications.

OCIS codes: (190.4420) Nonlinear optics, transverse effects in; (190.4400) Nonlinear optics, materials; (190.3100) Instabilities and chaos.

References and links

1. R. Knize, "Efficiency of degenerate four-wave mixing in two-level saturable absorbing medium," Opt. Lett. **18**, 1606-1608 (1993).
2. P. Miles, "Bottleneck optical limiters: the optimal use of excited-state absorbers," Appl. Opt. **30**, 6965-6979 (1994).
3. P. Miles, "Bottleneck optical pulse limiters revisited," Appl. Opt. **38**, 566-570 (1999).
4. T. Xia, D. Hagan, A. Dogariu, A. Said, and E. Stryland, "Optimization of optical limiting devices based on excited-state absorption," Appl. Opt. **36**, 4110-4122 (1997).
5. D. Kovsh, D. Hagan, and E. Stryland, "Numerical modeling of thermal refraction in liquids in the transient regime," Opt. Express **4**, 315-327 (1999). http://www.opticsexpress.org/abstract.cfm?URI=OPEX-4-8-315.
6. B. Justus, A. Houston, and A. Campillo, "Broadband thermal optical limiter," Appl. Phys. Lett. **63**, 1483-1485 (1993).
7. B. Justus, Z. Kafafi, and A. Huston, "Excited-state absorption-enhanced thermal optical limiting in C_{60}," Opt. Lett. **18**, 1603-1605 (1993).
8. F. Guo, W. Sun, D. Wang, and Y. Song, "Optical limiting of pentaazadentate complexes in solution for nanosecond pulses," Opt. Eng. **40**, 138-141 (2001).
9. M. Sanghadasa, I. Shin, R. Clark, H. Guo, and B. Penn, "Optical limiting behavior of octa-decyloxy metallo-phthalocyanines," J. Appl. Phys. **90**, 31-37 (2001).
10. J. Shirk, R. Pong, S. Flom, F. Bartoli, M. Boyle, and A. Snow, "Lead phthalocyanine reverse saturable absorption optical limiters," Pure Appl. Opt. **5**, 701-707 (1996).
11. J. Perry, K. Mansour, S. Marder, K. Perry, D. Alvarez, Jr., and I. Choong, "Enhanced reverse saturable absorption and optical limiting in heavy-atom-substituted phthalocyanines," Opt. Lett. **19**, 625-627 (1994).
12. I. Khoo, M. Wood, B. Guenther, M. Shih, P. Chen, Z. Chen, and X. Zhang, "Nonlinear optical liquid cored fiber array and liquid crystal film for ps-cw frequency agile laser optical limiting application," Opt. Express **2**, 471-482 (1998). http://www.opticsexpress.org/abstract.cfm?URI=OPEX-2-12-471.
13. I. Khoo, M. Wood, M. Shih, and P. Chen, "Extremely nonlinear photosensitive liquid crystals for image sensing and sensor protection," Opt. Express **4**, 432-442 (1999). http://www.opticsexpress.org/abstract.cfm?URI=OPEX-4-11-432

#2624 - $15.00 US Received June 20, 2003; Revised August 18, 2003

14. H.B. Lin, R.J. Tonucci and A.J. Campillo, "Two-dimensional photonic bandgap optical limiter in the visible," Opt. Lett. **23**, 94-96 (1998).
15. M. Scalora, J..P. Dowling, C.M. Bowden, and M.J. Bloemer "Optical Limiting and Switching of Ultrashort Pulses in Nonlinear Photonic Band Gap Materials," Phys. Rev. Lett. 73, 1368 (1994).
16. M.C. Larciprete, C.Sibilia, S. Paolini, M. Bertolotti, F. Sarto and M. Scalora," Accessing the optical limiting properties of metallo-dielectric photonic band gap structures," J. Appl. Phys. 93, 5013-5017 (2003).
17. J.S. Shirk, R.G.S. Pong, S.R. Flom, A. Hiltner and E. Baer, "Nonlinear nanolayered polymers: 1D photonic materials with applications to optical limiting, " Conference on Laser and Electro-Optics Europe – Technical Digest, 83-84 (2001).
18. G. D'Aguanno, M. Centini, M. Scalora, C. Sibilia, M. Bertolotti, M..J. Bloemer and C..M. Bowden, "Energy exchange properties during second-harmonic generation in finite one-dimensional photonic band-gap structures with deep gratings," Phys. Rev. E 67, 016606 (2003).
19. S. Hughes, G. Spruce, B. Wherrett, K. Welford, and A. Lloyd, "The saturation limit to picosecond, induced absorption in dyes," Opt. Commun. **100**, 113-117 (1993).
20. S. Hughes, J. Burzler, G. Spruce, and B. Wherrett, "Fast Fourier transform techniques for efficient simulation of Z-scan measurements," J. Opt. Soc. Am. B **12**, 1888-1893 (1995).
21. S. Hughes and B. Wherrett, "Multilevel rate-equation analysis to explain the recent observations of limitations to optical limiting dyes," Phys. Rev. A **54**, 3546-3552 (1996).
22. S. Hughes, "A novel computational technique for propagating picosecond, intense laser pulses through a multi-level system," Opt. Commun. **132**, 236-240 (1996).
23. S. Hughes, J. Burzler, and T. Kobayashi, "Modeling of picosecond-pulse propagation for optical limiting applications in the visible spectrum," J. Opt. Soc. Am. B **14**, 2925-2929 (1997).
24. C. Li, L. Zhang, M. Yang, H. Wang, and Y. Wang, "Dynamic and steady-state behaviors of reverse saturable absorption in metallophthocyanine," Phys. Rev. A **49**, 1149-1157 (1994).
25. J. Si, M. Yang, Y. Wang, L. Zhang, C. Li, D. Wang, S. Dong, and W. Sun, "Nonlinear absorption in metallo-porphyrin-like," Opt. Commun. **109**, 487-491 (1994).
26. C. Li, J. Si, M. Yang, R. Wang, and L. Zhang, "Excited-state nonlinear absorption in multi-energy-level molecular systems," Phys. Rev A **51**, 569-575 (1995).
27. X. Deng, X. Zhang, Y. Wang, Y. Song, S. Liu, and C. Li, "Intensity threshold in the conversion from reverse saturable absorption to saturable absorption and its application in optical limiting," Opt. Commun. **168**, 207-212 (1999).
28. J. W. Haus, B. Y. Soon, M. Scalora, M. Bloemer, C. Bowden, C. Sibilia, and A. Zheltikov, "Spatio-temporal instabilities for counter-propagating waves in periodic media," Opt. Express **10**, 114-121 (2002).
29. J. W. Haus, B. Y. Soon, M. Scalora, C. Sibilia, I. Mel'nikov, "Coupled-mode equations for Kerr media with periodically modulated linear and nonlinear coefficients," J. Opt. Soc. Am. B **19**, 2282-2291 (2002).
30. N. M. Lichinitser, C. J. McKinstrie, C. M. de Sterke, and G. P. Agrawal, ''Spatiotemporal instabilities in nonlinear bulk media with Bragg gratings,'' J. Opt. Soc. Am. B **1**8, 45–54 (2001).
31. C.M. de Sterke, D.G. Salinas and J. Sipe, "Coupled-mode theory for light propagation through deep nonlinear gratings," Phys. Rev. E **54**, 1969-1989 (1996).
32. M. Scalora and M. Crenshaw, "A beam propagation method that handles reflections," Opt. Commun. **108**, 191-196 (1994).
33. S. Yang, "Optimization of passive optical limiters," Ph.D. Dissertation, University of Central Florida, 2000.

1. Introduction

With the development of more powerful lasers for applications, such as, laser ablation and the air-borne laser, optical limiters may be needed to provide human eye and optical detector protection. In some instances, the light intensity is randomly fluctuating, such that the intensity is extremely high at times, and dims at other times. One option is to use a notch filter to remove a narrow band of wavelengths. However, wavelength agile lasers now available make this strategy useless. So, a smart optical limiter is needed that is transparent for low input intensities and clamps the throughput at high input intensities, and is effective over a wide band of wavelengths. The ideal solution would be a passive optical limiter with a fast response; since mechanical or electrical switches and controller circuits would not response fast enough to ultrafast pulse inputs.

There are various types of passive optical limiters and their optical limiting performance is based on a wide variety of nonlinear optical phenomena such as saturable [1] and reverse-saturable absorption [2-3], two-photon absorption, thermal lensing effect, optically-induced molecular reorientation in liquid crystals, *etc*. Passive optical limiters are becoming popular

#2624 - $15.00 US Received June 20, 2003; Revised August 18, 2003

with proven effectiveness for short pulses and CW with no additional electronic switches and controller circuits. Reverse-saturable absorption has been exploited as a good candidate for optical limiting action because it can lower the transmission further at higher intensity. An interesting improvement in optical limiter performance is to cascade optical limiters, which is commonly known as tandem optical limiters, so that each optical limiter prevents damage in the following one [2-4].

Thermal lensing effects to defocus intense light are broadband limiters [5-7]. Recent research seeks to improve optical limiting through new materials synthesis to create higher reverse-saturable absorption coefficients. Examples of this approach are pentaazadentate complexes in solution [8] and metallo-phthalocyanines [9-11], which possess high optical nonlinearity, good thermal stability and high excited-state absorption cross-sections. Still other candidates are nonlinear, photosensitive liquid crystals with large optical anisotropy and efficient molecular reorientation mechanisms [12-13]. Optical limiting in two-dimensional PCs was proposed and experimentally examined using a thermal nonlinearity [14]. Scalora *et al*. [15] first proposed one-dimensional PBG optical limiters based on a nonlinear shift of the band edge. Recently experimental results were reported in metallo-dielectric PCs [16] and polymers [17], as well as, a new type of optical limiter employing a pump depletion and reflection phenomenon in second-order materials [18].

In this paper, we present results on the optical limiting capability of a nonlinear, photonic crystal optical limiter. Optical limiting in our materials is based on the nonlinear, defocusing effect of the transverse modulational instability, which is a novel application of this phenomenon. By placing an aperture in the near-field or far-field high-intensity light can be filtered before entering the detector. In this paper we explore the roles played by the choice of the materials and the geometry of the photonic crystal, and discuss merits and demerits of the photonic crystal optical limiter.

2. Theory

In this section we first distinguish the intensity-dependent transmission characteristics between saturable (SA) and reverse saturable (RSA) absorbers. Next, a brief review will be presented of the spectral method that we will use to model pulse propagation in the photonic crystal. Finally, we will discuss a proposed standard measures to compare the performance of our optical limiter designs.

2.1 Saturable and reverse saturable absorption

One technique to create mode locking is to insert a saturable absorber in the cavity [18]. Probing the rate equations gives insight to the absorptive behavior of the material, which leads to the physical study of two-photon absorption, SA, and RSA. Earlier research established that SA and RSA phenomena have promising optical limiting capability, and therefore these mechanisms were quickly exploited in the field of optical limiting.

In the past decade, Hughes and co-workers [19-23] and the Harbin Institute of Technology's group [24-27] have published excellent studies elucidating our physical understanding of SA and RSA for selected materials. Briefly, we will use an example from Hughes *et al*. [21] to illustrate the transmission characteristic for both SA and RSA using a simple three-level model. Without consideration of vibrational and rotational levels, the three-level model is depicted in Fig. 1(a), where $S_i \ \forall\, i \in \{0,1,2\}$ is the electronic energy level, and σ_{01} and σ_{12} are the ground- and excited-state absorption cross-sections, respectively. Note that the relaxation lifetime of the ground- and excited-state is assumed to be minute, and thus ignored.

#2624 - $15.00 US Received June 20, 2003; Revised August 18, 2003

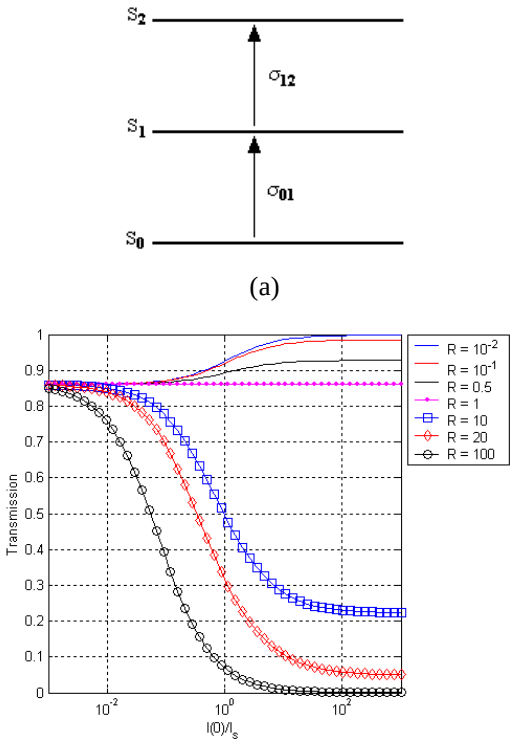

Fig. 1 The (a) three-level model; and (b) the plot of transmission versus incident irradiance (normalized by the saturation irradiance I_s).

With reference to Hughes *et al.*, the steady-state, three-level rate equations are solved to obtain the irradiance rate equation neglecting diffraction effects

$$\frac{dI(z)}{dz} = -\alpha_0 \left[\frac{I(z)R + I_s}{I(z) + I_s} \right] I(z), \tag{1}$$

where I is the irradiance, I_s is the saturation irradiance, $R=\sigma_{12}/\sigma_{01}$ is the ratio of excited-state and ground-state absorption cross-sections (depicted in Fig. 1(a)), α_0 is the linear absorption coefficient, and z is the propagation variable. Solving the first order partial differential equation in Eq. (1), we have a transcendental equation for the transmittance (T) given as

$$T = \frac{I(L)}{I(0)} = \exp(-\alpha_0 L) \left[\frac{I(L)R + I_s}{I(0)R + I_s} \right]^{(1-\frac{1}{R})}, \tag{2}$$

where *I(0)* and *I(L)* are the irradiances at the input and exit faces of the absorbing medium, respectively. Based on Eq. (2), curves of the transmission versus incident irradiance (normalized by I_s) are plotted in Fig. 1(b), where $\alpha_0 L = 0.15$ is assumed. At low irradiance $T \approx \exp(-\alpha_0 L)$ is observed for both SA (R<1) and RSA (R>1). As the incident irradiance is increased for SA, the transmission also increases. The opposite behavior is found for RSA, where the transmission decreases as the irradiance is increased. This case represents the optical limiting phenomenon for large values of the ratio R most of the incident light is absorbed at high irradiance. From Fig. 1(b), we see that using this model at high irradiance, when $R \leq 10^{-2}$, the SA transmission approach unity, and when $R \geq 100$, the RSA transmission is small.

#2624 - $15.00 US
Received June 20, 2003; Revised August 18, 2003

2.2 Photonic crystal evolution equations

In previous papers we applied the multiple scales method to the classical, nonlinear wave equation to derive a set of coupled-mode equations for the photonic crystal with homogeneous [28] and inhomogeneous Kerr nonlinearity [29]. An equivalent set of equations for homogeneous Kerr nonlinearity [30] and for inhomogeneous Kerr coefficients without transverse effects was derived by de Sterke *et al.* [31]. In our paper we studied modulation instabilities (MIs) and found that the inhomogeneous Kerr coefficients can either enhance or suppress the MI threshold intensity. The resulting coupled-wave equations are

$$\begin{aligned}\frac{1}{\upsilon}\frac{\partial E_f}{\partial t} = &-\frac{\partial E_f}{\partial z} + \frac{i}{F}\nabla_\perp^2 E_f + \left(i\delta - \frac{\alpha_0}{2}\right)E_f + \left(i\kappa_1 - \frac{\alpha_1}{2}\right)E_b \\ &+ i\eta_0\left(\left|E_f\right|^2 + 2\left|E_b\right|^2\right)E_f + i\eta_1\left(\left|E_b\right|^2 + 2\left|E_f\right|^2\right)E_b \\ &+ i\eta_{-1}E_f^2E_b^* + i\eta_2E_b^2E_f^*,\end{aligned} \tag{3a}$$

and

$$\begin{aligned}\frac{1}{\upsilon}\frac{\partial E_b}{\partial t} = &\frac{\partial E_b}{\partial z} + \frac{i}{F}\nabla_\perp^2 E_b + \left(i\delta - \frac{\alpha_0}{2}\right)E_b + \left(i\kappa_{-1} - \frac{\alpha_{-1}}{2}\right)E_f \\ &+ i\eta_0\left(\left|E_b\right|^2 + 2\left|E_f\right|^2\right)E_b + i\eta_{-1}\left(\left|E_f\right|^2 + 2\left|E_b\right|^2\right)E_f \\ &+ i\eta_1E_b^2E_f^* + i\eta_{-2}E_f^2E_b^*,\end{aligned} \tag{3b}$$

where E_f and E_b are the forward- and backward-propagating field amplitudes, respectively. Other symbols are defined as follows: z is the propagation direction, t is the time variable, υ is the group velocity, $\nabla_\perp^2$ is the transverse Laplacian operator, $\alpha_l\ \forall\{l \in 0,\pm1\}$ is the l^{th} Fourier coefficient of the absorption coefficient, $\kappa_m\ \forall\{m \in \pm1\}$ is the Fourier component of the coupling coefficient (proportional to the index contrast between the two layers), $\eta_n\ \forall\{n \in 0,\pm1,\pm2\}$ is the n^{th} Fourier coefficient of the third-order nonlinear Kerr coefficient, F is called the Fresnel number, and δ is the laser detuning from the center of the gap. The corresponding boundary conditions are

$$E_f(x,0,t) = S(x,z,t) = \left|S\right|\exp\left(\frac{-x^2}{\sigma_x^2}\right)\exp\left(\frac{-z^2}{\sigma_z^2}\right), \tag{3c}$$

and

$$E_b(x,L,t) = 0. \tag{3d}$$

Note that S is the peak value of the incident electric field, x is the transverse direction, σ_x^2 and σ_z^2 are the spatial variance of the incident Gaussian pulse in the respective x- and z-direction. We rewrite Eqs. 3(a-b) in a compact form so that we can code it using the spectral method, and we first arrange them in matrix form, given as

#2624 - $15.00 US Received June 20, 2003; Revised August 18, 2003

$$\frac{1}{v}\frac{\partial}{\partial t}\begin{bmatrix} E_f \\ E_b \end{bmatrix} = \left\{ \begin{bmatrix} -\frac{\partial}{\partial z}+\frac{i}{F}\nabla_\perp^2 + i\delta - \frac{\alpha_0}{2} & 0 \\ 0 & \frac{\partial}{\partial z}+\frac{i}{F}\nabla_\perp^2 + i\delta - \frac{\alpha_0}{2} \end{bmatrix} \right.$$

$$+ \begin{bmatrix} i\eta_0(|E_f|^2 + 2|E_b|^2) + 2i\eta_1 E_b E_f^* + i\eta_{-1} E_f E_b^* + i\eta_2 E_b^2 \frac{E_f^*}{E_f} & i\eta_1 |E_b|^2 \\ i\eta_{-1}|E_f|^2 & i\eta_0(|E_b|^2 + 2|E_f|^2) + 2i\eta_{-1} E_f E_b^* + i\eta_1 E_b E_f^* + i\eta_{-2} E_f^2 \frac{E_b^*}{E_b} \end{bmatrix}$$

$$\left. + \begin{bmatrix} 0 & -i\kappa_1 - \frac{\alpha_1}{2} \\ -i\kappa_{-1} - \frac{\alpha_{-1}}{2} & 0 \end{bmatrix} \right\} \begin{bmatrix} E_f \\ E_b \end{bmatrix}. \qquad (4)$$

We denote that the first, second, and third matrices in the curly bracket on the right-hand side of Eq. 4 as the ***L***, ***N***, and ***K*** operators, respectively.

The spectral method was introduced in the 1970s, and has become a useful numerical technique to solve a wide range of physics and engineering computational problems. Many modifications are made to the spectral method so that it remains robust for different scenario. For example, Scalora *et al.* showed a version of the spectral method that can handle transmission, diffraction, and reflection of the pulse propagation [32]. A coupled-mode version of the spectral method was introduced where the transmission and reflection are separated in the solution space [28]. Recently, an improved version of the spectral method was demonstrated that includes the periodically modulated linear and nonlinear coefficients [29].

Using the conventional split-steps formalism of the spectral method (e.g, $\frac{\partial U}{\partial t} = (H + J)U$ has the approximate solution given as $U(t+\Delta t) \approx \exp(\Delta t H/2)\exp(\Delta t J)\exp(\Delta t H/2)U(t)$). For our case we use the approximation: $\exp[\Delta t(\boldsymbol{L}+\boldsymbol{N}+\boldsymbol{K})] \approx \exp(\Delta t\boldsymbol{L}/2)\exp(\Delta t\boldsymbol{K}/2)\exp(\Delta t\boldsymbol{N})\exp(\Delta t\boldsymbol{K}/2)\exp(\Delta t\boldsymbol{L}/2)$, ***L***, ***N***, and ***K*** are defined above. The electric field has the solution

$$\frac{1}{v}E(t+\Delta t) = \exp(\Delta t\boldsymbol{L}/2)\exp(\Delta t\boldsymbol{K}/2)\exp(\Delta t\boldsymbol{N})\exp(\Delta t\boldsymbol{K}/2)\exp(\Delta t\boldsymbol{L}/2)E(t). \qquad (5)$$

Since diagonal matrices commute, we let $\boldsymbol{N}$=diag($\boldsymbol{N}$)+($\boldsymbol{N}$-diag($\boldsymbol{N}$))=$\boldsymbol{N}_{\mathrm{d}}$+$\boldsymbol{N}_{\mathrm{od}}$ (where $\boldsymbol{N}_{\mathrm{d}}$=diag($\boldsymbol{N}$), $\boldsymbol{N}_{\mathrm{od}}$= $\boldsymbol{N}$-diag($\boldsymbol{N}$), and the subscripts 'd' and 'od' refer to the diagonal and off-diagonal, respectively), and the approximated exponential of a matrix expansion of ***N*** is given as

$$\exp(\Delta t\boldsymbol{N}) \approx \exp(\Delta t\boldsymbol{N}_{\mathrm{d}}) + \Delta t\boldsymbol{N}_{\mathrm{od}}, \qquad (6)$$

where the exponential expansion of $\boldsymbol{N}_{\mathrm{od}}$ includes only the first term in the expansion. Second- and higher-order terms can be added in Eq. (6) by continuing the expansion of the exponential to higher orders.

One factor in our spectral method is the parameter η_n, which we use to tweak the duty cycle of the photonic crystal. For example, if the respective lengths along *z* of first and second materials are 'a' and 'b' such that a+b=d, we define the duty cycle (DC) to be DC=(a/d)x100%. We now illustrate an arbitrary case that we will use for the numerical simulation such that first and second materials have $\frac{2\pi\omega^2}{kc^2}\chi^{(3)}$ to be *1+i* and *1*, respectively.

To relate the scaled units to physical quantities consider a sample made from two dielectrics with dielectric contrast, *0.01* and a nonlinear optical coefficient $n_2 = 10^{-10}\ cm^2/W$, the corresponding MI threshold intensity ($|S| \sim 0.3$) in finite systems is about *3 MW/cm²* (for a

#2624 - $15.00 US Received June 20, 2003; Revised August 18, 2003

10 ns pulse width this corresponds to a fluence around *3 mJ/cm*^{2}). At threshold the nonlinear change of the index is about *0.0003*. In the simulations performed here our sample length is about *120* layers or *30* wavelengths thick. If the average refractive index is *1.5*, the sample has a thickness around *12 μm*. Our maximum input fluence levels are about ten times larger than the threshold values. These values are far below the damage threshold for most materials.

We use the Fourier transform pair to compute the Fourier series coefficients, given as

$$p(z) = \sum_{s=-\infty}^{\infty} P_s \exp(2\pi i s z / d), \tag{7a}$$

and

$$P_s = \frac{1}{d}\int_0^d p(z)\exp(-2\pi i s z / d)\, dz, \tag{7b}$$

where P_s is a Fourier coefficient of the periodic function $p(z)$, s indexes the frequency variable, and d is the period. Depending on the function that we want to synthesize, we may need infinite Fourier coefficients to obtain an accurate synthesis.

2.3 Figures of Merit for fair evaluation of the Optical Limiter Performance

In order to compare different optical limiter designs, we impose standard figures of merit for fair comparison of the optical limiter performance. First, we define the characteristics of an "ideal optical limiter", so that we can have a set of guidelines. An ideal optical limiter's transmission characteristic is similar to an ideal low-pass filter depicted in Fig. 2 as the red dotted curve. The transmission pass- and reject-bands are unity and zero, respectively, with a sharp cutoff. Imagine the optical data communication scenario, when the detector is jammed or damaged, the ideal optical limiter forbids intensities above the preset threshold from reaching the detector, thus saving the detector and avoids detecting corrupted data. The empirical transmission curve will deviate from the ideal such as the transmission curve shown as the blue solid curve in Fig. 2. We see that T_{max} is not at unity and T_{min} is not at zero. Also, the cutoff point is said to be the $T_{50\%}$ point where there is a gradient of transmission around the cutoff point.

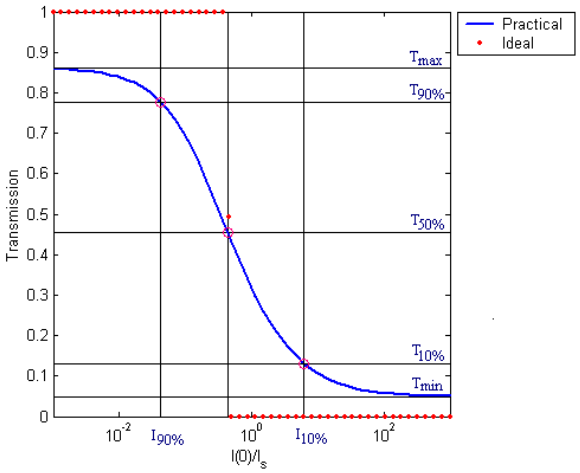

Fig. 2. The transmission curve of an ideal optical limiter.

There are three figures of merit that we use to define to categorize the performance of optical limiters. First, we define the transmission contrast ratio (TCR) as

$$\mathrm{TCR} = \frac{T_{max} - T_{min}}{T_{max} + T_{min}} \times 100\% = \frac{1 - (1/\psi)}{1 + (1/\psi)} \times 100\%, \tag{8}$$

#2624 - $15.00 US
Received June 20, 2003; Revised August 18, 2003

where ψ is the ratio of T_{max}/T_{min}. We see that if T_{min} is zero, TCR will be unity for any non-zero T_{max}. Next, we define the transmission dynamic range (TDR) to be

$$\mathrm{TDR} = \frac{T_{max}}{T_{min}} = \psi. \tag{9}$$

We notice that if T_{min} is zero, TDR is infinity for any non-zero T_{max}. For example, let's say T_{min} is 0.001. If T_{max} is 0.95, TCR=0.9979 and TDR=950. If T_{max} is 0.90, TCR=0.9978 and TDR=900. We see that TDR is more sensitive to the change in T_{max}. However, for a non-zero T_{min}, it is easier to see that TCR is approaching unity rather than to distinguish between large numbers. We define a the transmission cutoff (TCO) response band proportional to the intensity difference between the 10% and 90% transmission points

$$\mathrm{TCO} = \left| \frac{I_{90\%} - I_{10\%}}{I_{90\%} + I_{10\%}} \right|. \tag{10}$$

For example, bottleneck and tandem optical limiters use cascaded optical limiters design to obtain multiple dips in transmission to achieve low transmission at high intensity [2-3, 33]. In this manner each element doesn't demand a large TCO. Ideally speaking, for the entire system we want TCR=1, $\mathrm{TDR} \to \infty$, and TCO=0. The reflected light from a PC limiter has an analogous set of performance criteria replacing the letter 'T' by 'R' for 'reflection' (i.e., RCR, RDR, RCO). The reflection could likewise be used for designing efficient optical limiting action, although we do not explore that possibility here.

3. Numerical results

The most important point we want to consider is whether the PC optical limiter is better than an optical limiter made of only homogeneous nonlinear material. We assume that the both optical limiters are illuminated by collimated light and the corresponding transmission and reflection is probed using detectors at a far field point (i.e. the Fraunhofer regime) with an aperture placed in front of the detector. The aperture size is controlled and is proportional to the transverse pulse width. For example, if the aperture size is 40% opened, the aperture size is full width at 40% maximum of the incident transverse pulse width at the front face of the optical limiter. Obviously, aperture size of 0% and 100% refer to fully closed and opened apertures, respectively. For homogeneous and PC optical limiters, we use an incident Gaussian pulse scaled so that $\sigma_x^2 = \sigma_z^2 = 1$ and the Fresnel number is *F=100*, unless stated otherwise. The laser detuning δ is set to 1.12 (the first transmission maximum for normal dispersion) for all cases discussed later.

The figures of merit for both optical limiters of various aperture sizes are tabulated in Table 1(a-b). From Table 1, we deduce that the performance in terms of TCR, TDR, and TCO of the homogeneous material optical limiter generally lags behind that of the PC optical limiter, except when the aperture is open. Even a 90 % open aperture improves the performance of the PC optical limiter in all criteria. While the use of the aperture greatly improves the PC limiter performance, there is a trade off in throughput. A balance between throughput and optical limiting behavior is required in making usable devices. Of course, the homogeneous nonlinear optical limiter has no reflection, and therefore there is no possible comparison made with the PC optical limiter reflection criteria. However, the corresponding reflection criteria are comparable to the transmission criteria of the homogeneous optical limiter.

The corresponding plots of output fluence (E_{out}) versus input fluence (E_{in}) and transmission and reflection curves are depicted in Figs. 3(a-b), respectively. Note $E_{in}=800$ corresponds to a Gaussian input with amplitude $|S|=1$. The curves are plotted for each of the apertures sizes listed in Table 1. The absolute transmission of the homogeneous optical limiter is higher than the PC one.

#2624 - $15.00 US Received June 20, 2003; Revised August 18, 2003

Table 1. The Figures of merit of (top) the homogeneous nonlinear optical limiter with third order Kerr nonlinearities of 1+0.5i; and (bottom) the photonic crystal optical limiter with DC=20% and third order Kerr nonlinearities of 1+i and 1 for the respective first and second materials.

Aperture Size (%)	TCR (%)	TDR	TCO
100	29.2	1.8	0.8
90	29.7	1.8	0.8
79	29.6	1.8	0.8
61	28.8	1.8	0.8
50	28.1	1.8	0.8
38	27.4	1.8	0.8
26	26.6	1.7	0.8
16	25.8	1.7	0.8
7	25.2	1.7	0.8
2	24.8	1.7	0.8

Aperture Size (%)	TCR (%)	TDR	TCO	RCR (%)	RDR	RCO
100	4.5	1.1	0.7	20.1	1.5	0.8
90	30.0	1.9	0.4	24.1	1.6	0.8
79	36.7	2.2	0.4	24.6	1.7	0.8
61	42.4	2.5	0.4	24.5	1.6	0.8
50	44.3	2.6	0.4	24.1	1.6	0.7
38	45.6	2.7	0.4	23.6	1.6	0.7
26	46.2	2.7	0.4	23.0	1.6	0.7
16	46.4	2.7	0.4	22.4	1.6	0.7
7	46.4	2.7	0.4	21.9	1.6	0.7
2	46.2	2.7	0.4	21.5	1.5	0.7

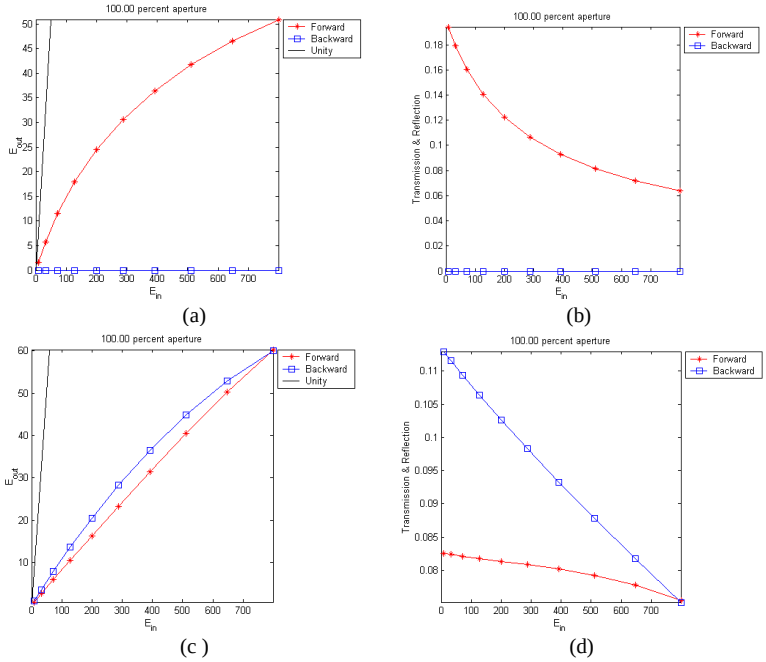

Fig. 3. The animated plots of (a) transmitted/reflected output fluence versus input fluence and (b) transmission/reflection curve of the homogeneous nonlinear optical limiter with third order Kerr nonlinearities of 1+0.5i; and (c) transmitted/reflected output fluence versus input fluence and (d) transmission/reflection curve of the photonic crystal optical limiter with DC=20% and third order Kerr nonlinearities of 1+i and 1 for the respective first and second materials.

#2624 - $15.00 US Received June 20, 2003; Revised August 18, 2003

Figures 3(a-d), demonstrate that the homogeneous nonlinear optical limiter with aperture effect has higher T_{max}, and also higher T_{min}. On the other hand, the photonic crystal optical limiter has lower T_{max}, and also lower T_{min}. Both optical limiters have transmission characteristics similar to Fig. 1 when R > 1, when RSA is the absorption mechanism. Imagine that incident intensity gradually increases; the homogeneous nonlinear optical limiter absorbs energy that must be dissipated. The PC optical limiter uses linear index changes for reflection, nonlinear index changes for the modulation instability, and nonlinear absorption for optical limiting; they share in the task of reducing transmission at all intensities and reduce the heat load on the sample.

To compare the two cases, assume both optical limiters transmit 60% at a high intensity; the homogeneous nonlinear optical limiter absorbs transmit 40%. On the other hand the PC optical limiter reflects a portion of the incident energy and the transmitted 60 % has a diffracted phase front and thus it serves as a better optical limiter. The purpose of the aperture is to clip the transverse structure as it breakups due to modulational instabilities; this gives a large improvement in the optical limiting performance. Comparing performance between these two optical limiters, the PC optical limiter has several specific merits.

The PC optical limiter also filters incoming radiation by reflecting a portion of it. Tuning the light to the transmission maximum and using long pulses eliminates the linear transmission loss. The PC naturally filters short pulses whose spectrum lies within the band gap or near the band edge. Our studies show that strong limiting action of the device extends away from the band edge to about the third transmission maximum. This is about 50 % of the band gap width in our example. The stronger the index variation used for the two materials, then the wider the bandwidth becomes.

Now, we explore the role played by the choice of nonlinear materials for the PC optical limiter. For DC=20%, we choose the first and second materials' third-order Kerr nonlinearities as 1 and 1+0.5i, respectively. The first layer is the high linear refractive index medium. The figures of merit listed in Table 2 show a much more moderate improvement with aperture size when compared against the results in Table 1. Comparing the figures of merit of the two photonic crystal optical limiters with aperture effect, we observe that when the Kerr nonlinearity of the first material is complex, it yields better TCR, TDR, TCO, and RCO as compared to when the second material is complex. Thus, by engineering the correct choice of materials, further optimization of the PC optical limiter performance is possible. This is due to the concentration of the electric field in the low index medium at the upper band edge. A strong part of the optical limiting action is due to the field enhancement affect on the absorption, as we previously discussed for the case of linear absorption [28]. Note that numerically, we can always tweak η_n to obtain the optimized optical limiter performance, but the Kerr nonlinearities may not be physically realizable. Thus, the optical limiter designer must keep in mind the realistic choice of materials.

Table 2. The figures of merit of photonic crystal optical limiter of respective first and second materials' Kerr nonlinearities as 1 and 1+0.5i.

Aperture Size (%)	TCR (%)	TDR	TCO	RCR (%)	RDR	RCO
100	38.2	2.2	0.9	32.7	2.0	0.8
90	40.4	2.4	0.9	33.2	2.0	0.8
79	41.2	2.4	0.9	32.9	2.0	0.8
61	41.2	2.4	0.9	32.0	1.9	0.8
50	40.7	2.4	0.8	31.2	1.9	0.8
38	40.1	2.3	0.8	30.4	1.9	0.8
26	39.2	2.3	0.8	29.5	1.8	0.8
16	38.4	2.2	0.8	28.7	1.8	0.8
7	37.7	2.2	0.8	28.1	1.8	0.8
2	37.1	2.2	0.8	27.6	1.8	0.8

We also examine the role played by the geometry of the photonic crystal optical limiter, i.e. we change the duty cycle of each material in the two-layer period. For the case, where the

#2624 - $15.00 US Received June 20, 2003; Revised August 18, 2003

Kerr nonlinearities are 1+i and 1 for the respective first and second materials, their corresponding transmission curves for various DC∈ {0,10,20,...,100} at aperture size of 100% and 50%, respectively, are depicted in Figs. 4(a-b).

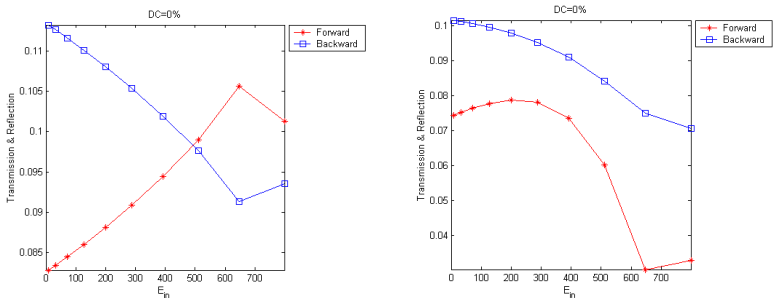

(a) (b)

Fig. 4. The animated transmission curves for various DC for aperture size of (a) 100%; and (b) 50%.

When DC is around 20~30%, we have an 50% aperture size outperforming 100% aperture size with better optical limiting performance in all respects: smaller TCO (or RCO) and improved TCR (or RCR) and TDR (or RDR) with low T_{min}. Note that when the DC is gradually increased for the case of 100% aperture size, the effective absorption mechanism changes from SA to RSA with a sudden dip in transmission. Thus, we find that there is a DC that optimizes the optical limiting performance.

Finally we note that by using a longer incident pulse, the linear reflection coefficient of the pulse is reduced. This can improve the absolute performance of the device. We stretch the Gaussian pulse by adding a long plateau at the maximum of the Gaussian pulse; the same pulse height was used for our stretched version of the original Gaussian pulse. The corresponding results are depicted in Fig. 5 for various DC at 100% and 50% aperture sizes, and the corresponding figures of merit are tabulated in Table 3 for DC of 20%. Note that the TDR shows a dramatic improvement over our results in Table 1. The increase is nearly one order of magnitude. In cases where a narrow band of light is expected, the limiter naturally filters short pulses and then has improved performance filtering intense, long pulses.

Table 3. The figures of merit of photonic crystal optical limiter of respective first and second materials' Kerr nonlinearities as 1+i and 1 with the elongated version of the original Gaussian pulse.

Aperture Size (%)	TCR (%)	TDR	TCO	RCR (%)	RDR	RCO
100	41.0	2.4	0.5	40.3	2.4	0.8
90	80.3	9.1	0.8	63.5	4.5	0.8
79	83.8	11.4	0.8	64.2	4.6	0.8
61	86.6	13.9	0.8	64.0	4.6	0.8
50	87.7	15.3	0.8	63.6	4.5	0.8
38	88.6	16.4	0.7	62.9	4.4	0.8
26	89.1	17.3	0.7	62.1	4.3	0.8
16	89.3	17.7	0.7	61.2	4.2	0.8
7	89.4	17.8	0.7	60.5	4.1	0.8
2	89.3	17.7	0.7	60.0	4.0	0.8

Contrasting our findings illustrated in Fig. 4 for a short pulse, we examine a long-pulse in Fig. 5 using an initially stretched Gaussian pulse; the low intensity transmission is increased due to the smaller pulse bandwidth. We also observe improvements in all figures of merit except TCO, which is larger but comparable to the homogeneous optical limiter. If the incident pulse approaches a CW beam, the T_{max} will be even higher, thus further improve the optical limiting performance. The improved performance is attributed to the top-hat feature of the pulse where most of the energy has an intensity that lies above the MI threshold.

#2624 - $15.00 US Received June 20, 2003; Revised August 18, 2003

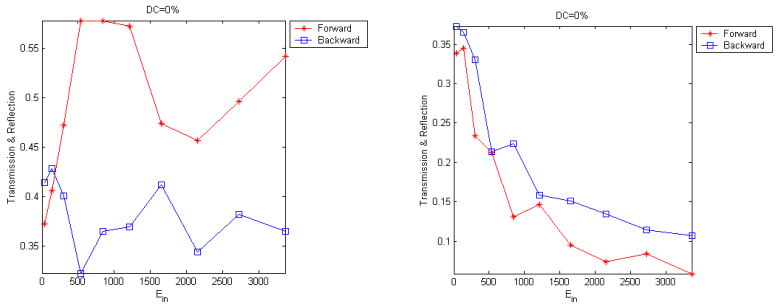

(a) (b)

Fig. 5. The animated transmission curves for elongated incident Gaussian pulse for various DC for aperture size of (a) 100%; and (b) 50%.

4. Conclusion

We studied the transmission characteristics of the PC optical limiters based on modulational instabilities, rather than the traditional nonlinear, band-edge shifting effect. In our investigation, we found that the PC optical limiter for short pulses improves the performance of the nonlinear material over that of the homogeneous nonlinear optical limiter. An aperture is used to take advantage of the transverse pulse breakup due to modulational instability and further reduce transmission at high intensity. For both short and long incident pulses, the PC optical limiter shows promising optical limiting characteristics. The performance of the photonic crystal optical limiter can be optimized by the choice of the materials and the geometry of the photonic crystal, where the optimization would be good for future work. The bandwidth of the optical limiting action is limited to wavelengths that are close to the band edge. We have found improved characteristics over a wavelength region that is about 50% of the band gap bandwidth. By using a large index contrast this can be extended to about a 100 nm band.

In Section 2 we considered a set of physical parameters that can be used to guide the experiments. For a dielectric contrast, *0.01* between the two materials, *10 ns* pulse widths, and a nonlinear optical coefficient $n_2 = 10^{-10}\ cm^2/W$, the corresponding threshold fluence for our simulations is around $3\ mJ/cm^2$. At threshold the nonlinear change of the index is about *0.0003*, which is several orders of magnitude smaller than required for thermal defocusing alone. The corresponding sample thickness is very thin around $12\ \mu m$. Our highest scaled input fluence *800* corresponds to a physical fluence around $30\ mJ/cm^2$.

Finally we note that there are other parameters that can be exploited to improve the performance of PC optical limiters. For instance, by focusing the light at the input face and by decreasing the Fresnel number the initial wave vectors are off-axis and susceptible to amplification by the MI phenomenon. The improved performance of the PC over a homogeneous material is a basis for further analysis and exploration of this new class of PBG optical limiters based on modulational instability. The optical limiters we propose are simpler to fabricate than their multi-dimensional counterparts. One-dimensional structures are routinely fabricated by a number of methods, for instance by sputtering, multi-layer polymer extrusion, or block co-polymer self-assembly, and they are cost effective and compact.

Acknowledgments

This work was supported by grants from the National Science Foundation: ECS-9630068 and ECS-0140109.